Recombination in plasma-deposited amorphous Si:H. Luminescence decay

C. Tsang* and R. A. Street
Xerox Palo Alto Research Center, 3333 Coyote Hill Road, Palo Alto, California 94304
(Received 27 November 1978)

An investigation of the photoluminescence decay in plasma-deposited amorphous Si:H is presented. The relative contribution of radiative and nonradiative transitions are shown in undoped samples with efficiencies varying over two orders of magnitude. In high-efficiency samples the 10-K radiative rate spans nearly six orders of magnitude, and is interpreted as radiative tunneling of band-tail electrons and holes. A systematic shift of time-resolved spectra by 0.15 eV to low energy is related to the width of the band tails. The decay is found to be excitation-intensity-dependent when the electron-hole pair density exceeds about 1.5×10^{18} cm^{-3}. This result is explained by overlap between neighboring pairs, and we deduce that the radius of the larger carrier is 11 Å $\pm$ 20%. A decrease of the radiative transition rate as the temperature increases is seen as evidence of carrier diffusion and is believed to explain a corresponding increase in the luminescence intensity. From this and other evidence it is argued that the electron-phonon coupling observed in the luminescence is associated with hole states, while electrons are not strongly coupled. We suggest that self-trapped hole states are split off from the top of the valence band, and account for the E_γ band in the field-effect density of states.

I. INTRODUCTION

Hydrogenated amorphous silicon prepared by plasma decomposition of SiH_4 generally exhibits photoluminescence.[1-4] The efficiency depends on the details of sample preparation and is largely determined by the density of singly occupied localized states in the band gap.[4] These defect states act as nonradiative centers and quench the luminescence when their density exceeds about 10^{17} cm^{-3}. The luminescence spectrum is usually a broad band centered near 1.4 eV with a width of 0.2–0.3 eV. A strong electron-phonon coupling is responsible for much of the spectral line width,[5] although a distribution of zero-phonon energies has been identified,[6] and is discussed further in this paper. The luminescence is generally attributed to transitions between conduction and valence bands, involving localized states at the band edges and this model is adopted here.[1,5] The evidence for this view is discussed elsewhere,[1,6] and is based on the luminescence energy, the density of states, and the luminescence excitation spectrum. While it can be established that transitions occur from states near the band edges, it is difficult to deduce the detailed origin of the states. For example it has been proposed that hydrogen provides the radiative centers.[3,7] This suggestion is not necessarily incompatible with the tail-state model, since Si-H antibonding states possibly form the bottom of the conduction band.[8] An alternative model assumes that luminescence is a donor-acceptor pair transition.[9] However if unintentional doping is involved, we believe that the reproducibility of the data in different samples, and the systematic trends with the deposition variables, would be difficult to explain.

Previous measurements of the luminescence decay identified both radiative and nonradiative components.[10] The radiative decay was reported to have a lifetime of ~30 μsec, whilst nonradiative recombination introduces a fast decay component with a lifetime less than 10 μsec. The relative magnitude of these components was shown to correlate with the relative luminescence efficiency in a series of doped and undoped samples. The observation of both radiative and nonradiative components in a sample was interpreted using a model in which the electron-hole pair is immobile after thermalization at low temperature. The resulting decay then depends on whether the pair is sufficiently close to a defect state in the gap for nonradiative capture to occur before radiative recombination. A random distribution of nonradiative centers could then explain both the observed decay data, and the dependence of luminescence efficiency on the density of singly occupied states in the gap observed by ESR.[4]

The present paper extends these preliminary results. The luminescence decay is investigated more thoroughly in undoped samples (Sec. III A) and is extended to much longer decay times (~10 msec compared to 50 μsec) in Sec. III B. We describe the spectral dependence of the decay through time-resolved measurements in Sec. III C, and the intensity dependence in Sec. III D. The temperature dependence of both the decay and the cw luminescence spectrum is given in Sec. III E. From the data we infer the distribution of zero-phonon energies that contribute to the luminescence. We also obtain an estimate of the wave-function extent of the carriers, and show that recombination by

radiative tunnelling is the most plausible interpretation of the data. We also discuss the influence and temperature dependence of carrier diffusion on the recombination. Finally, based on the discussion of the data presented here we propose a new interpretation of the reported density of localized states in the gap of a-SiH.

II. EXPERIMENTAL TECHNIQUES

The samples used in this study are prepared by plasma decomposition of SiH_4, using a capacitative reactor system described elsewhere.[4,11] By changing the deposition conditions, samples of varying luminescence efficiency are produced.[4] Most of this study uses samples of the highest quantum efficiency that we have currently obtained. These are prepared using low rf power in the plasma (1 W), and undiluted SiH_4. Other samples are used as indicated in the text.

Time-resolved luminescence is measured by a variety of techniques. Gated photon counting, with an S-1 photomultiplier as a detector, is used for luminescence energies above 1.2 eV. The time resolution of the detection is ~10 nsec. Lower luminescence energies are detected with a Si photodiode which has a time resolution of ~1 μsec. Pulsed excitation is by an acousto-optic modulator, either within the laser cavity, giving 20-nsec pulses, or outside the cavity when longer pulses are required. The 5145-Å line of an Ar^+ laser is used for excitation.

Separate apparatus was generally used for measuring cw luminescence spectra and its temperature dependence. In this case a cooled PbS detector and a Kr^+ laser excitation source was used. The spectra are all normalized for the throughout of the detection system. After normalization both sets of apparatus give essentially identical spectra, the discrepancy in the peak position being only 10-20 meV.

The luminescence decay is nonexponential, and it is convenient to analyze the data by a distribution $G(\tau)$ of decay times τ.[12] Under these circumstances the luminescence decay is a function of the duration of the excitation pulse, and this must be considered in analyzing the data. If $G(\tau)$ is the relative probability distribution that an electron-hole pair of radiative lifetime τ is generated for a particular excitation condition, then the density of such pairs $N(\tau, T)$ generated at the end of a pulse of length T is

$$N(\tau, T) = \text{const}\, G(\tau)\tau[1-\exp(-T/\tau)]. \quad (1)$$

The luminescence intensity of this population, at time t after excitation ceases, is given by

$$I(t, \tau, T) = \text{const}\,\tau^{-1}N(\tau, T)\exp(-t/\tau). \quad (2)$$

Thus for the distribution $G(\tau)$ the decay is

$$I(t, T) = \text{const}\int_0^\infty G(\tau)\left[1-\exp\left(\frac{-T}{\tau}\right)\right]\exp\left(\frac{-t}{\tau}\right)d\tau. \quad (3)$$

For an arbitrarily short T, the decay reduces to

$$I(t) = \text{const}\,T\int_0^\infty \tau^{-1}G(\tau)\exp\left(\frac{-t}{\tau}\right)d\tau. \quad (4)$$

It is usual to measure the decay under these conditions of a very short excitation pulse. However, if T falls within the distribution of lifetimes, then Eq. (3) can be approximated by

$$I(t, T) = \text{const}\left[\int_{\tau<T} G(\tau)\exp\left(\frac{-t}{\tau}\right)d\tau + T\int_{\tau>T}\tau^{-1}G(\tau)\exp\left(\frac{-t}{\tau}\right)d\tau\right]. \quad (5)$$

In this case it can be seen that the short lifetime components, in the first term, are suppressed by a factor τ/T compared to the longer components in the second term. Furthermore when $t \geq 5T$ the exponential makes the contribution from the first term negligible, and Eq. (5) reduces to the expression for a very short pulse for that portion of $G(\tau)$ with $\tau \geq 5T$. These results are used experimentally. A series of measurements are performed with an increasing time scale of both the excitation pulse and the measurement time. The complete response to a short excitation pulse can then be reconstructed from the data. Typically ten sets of data are used covering a time span of six decades (10^{-8}–10^{-2} sec). This method allows the observation of the decay to much longer times than is possible using very short pulses, because the fast components of the decay can be suppressed.

An interesting feature of Eq. (5) is that if $G(\tau)$ is a slowly varying function then the form of the decay depends only on the relative magnitude of t/T. Figure 1 shows an illustration of this effect

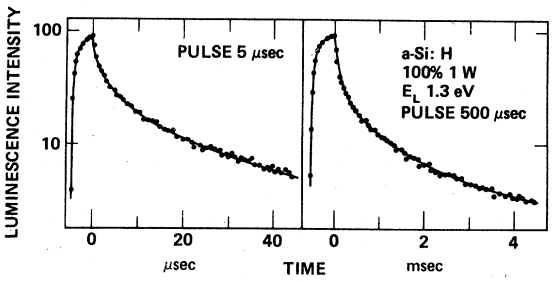

FIG. 1. Examples of the luminescence decay of an a-Si:H sample at 10 K illustrating that a broad distribution of decay times results in an apparent time dependence that varies with the excitation pulse length. E_L is the luminescence energy.

in the luminescence decay of a-Si:H. The two sets of data shown look almost identical despite having time scales differing by two orders of magnitude. This result shows how misleading decay data can be when $G(\tau)$ has a broad distribution. Another example of the suppression of the short time components is a comparison of Figs. 4 and 7. The latter shows the response to a very long excitation pulse (5 msec). Compared to the data of Fig. 4, the short time constant components are suppressed by about five orders of magnitude.

We obtain the distribution function $G(\tau)$ from the data by an iterative procedure. If $G(\tau)$ is a slowly varying function of τ then Eq. (4) can be approximated by

$$I(t) = \text{const} T \int_t^\infty \tau^{-1} G(\tau) \exp\left(\frac{-t}{\tau}\right) d\tau, \tag{6}$$

from which is obtained

$$\frac{dI}{dt} = \text{const}\, t^{-1} G(t)$$

or

$$G(t) = \text{const}\, I \frac{(d \ln I)}{(d \ln t)} \quad . \tag{7}$$

We therefore construct a third-order polynominal in lnI vs lnt to solve for $G(t)$ with starting values given by the experimental values of the quantities in Eq. (7). Equation 4 is then integrated using this $G(t)$ and the result is compared to the experimental $I(t)$. The polynominal parameters are then adjusted until a good fit to the data is obtained. From $G(\tau)$ the mean lifetime $\bar{\tau}$ can be evaluated from

$$\bar{\tau} = \int \tau G(\tau) d\tau / \int G(\tau) d\tau \ . \tag{8}$$

We note that if $I(t) \sim t^{-\beta}$ (with β slowly varying in time) then from Eq. (7), $\tau G(\tau) \sim \tau^{1-\beta}$. Thus the maximum contribution to the decay is expected to occur near $\beta = 1$. Figure 4 shows that this is observed.

III. EXPERIMENTAL RESULTS

A. Samples of different luminescence efficiency

Previous measurements on doped and undoped a-Si:H found that nonradiative recombination gave a fast initial decay of luminescence, and the magnitude of this decay correlated with the relative quantum efficiency.[10] That data included only two undoped samples. In Fig. 2 we show similar data for a larger selection of undoped samples which have quantum efficiencies varying by nearly two orders of magnitude. The different samples result from varying the deposition conditions. The

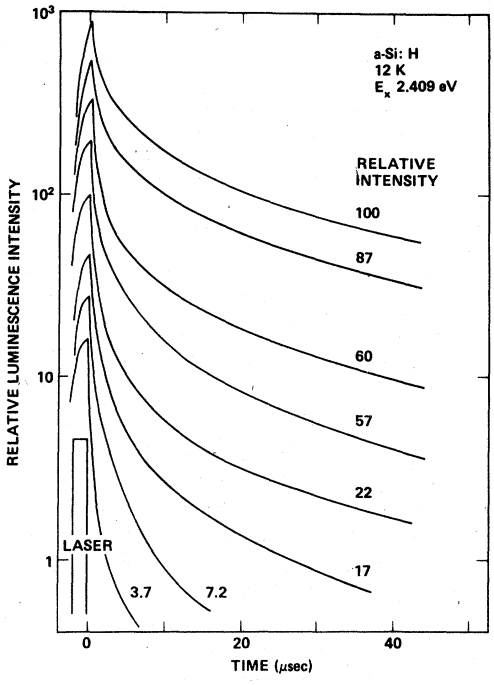

FIG. 2. Luminescence decay of various samples with differing deposition conditions. The relative intensities noted on the figure refer to the normalized cw luminescence intensity of the different samples. E_x is the excitation energy.

presence of a fast decay that increases as the efficiency decreases, and a slow component that is practically independent of the efficiency, is clearly evident. As before we obtain the relative strength of the two components by extrapolating the intensity of the slow decay back to $t = 0$, and comparing it with the initial intensity. The ratio of these values is plotted in Fig. 3 against the rela-

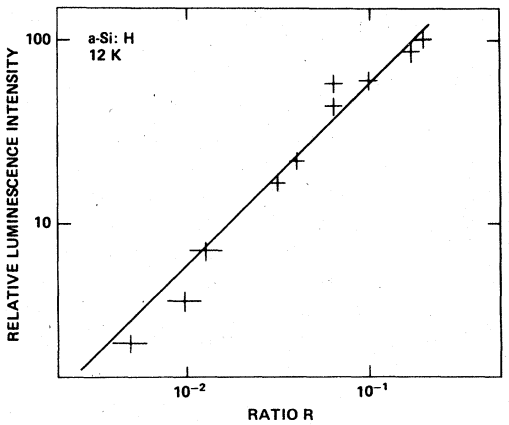

FIG. 3. Plot showing a linear relation between the cw luminescence intensity and the relative magnitude of the slow and fast decay. R is the intensity obtained by extrapolating the decay at 20–40 μsec back to $t = 0$, divided by the actual $t = 0$ value, in the data of Fig. 2.

tive luminescence intensity. The observed linear relationship is in agreement with our previous interpretation of the nonradiative transition in terms of tunneling to defect states.[10]

In order to investigate the radiative recombination it is advantageous to minimize the nonradiative component of the decay. For this reason most of the experimental results refer to a single sample that had the maximum observed efficiency. This sample was deposited with low rf power (1 W) and undiluted SiH_4 (100%). The absolute quantum efficiency of this sample was estimated by measuring the luminescence intensity with a calibrated power meter, and correcting for the collection optics of the apparatus. In this way we obtain a maximum quantum efficiency of 50%–100%. This maximum is observed at ~50 K and is about twice the intensity at 10 K (see Sec. III E). Thus the low-temperature efficiency is estimated at 25%–50%.

B. Luminescence decay

Figure 4(a) shows some examples of the luminescence decay following a short excitation pulse (the minimum pulse length used in 20 nsec) at different temperatures. As described in Sec. II,

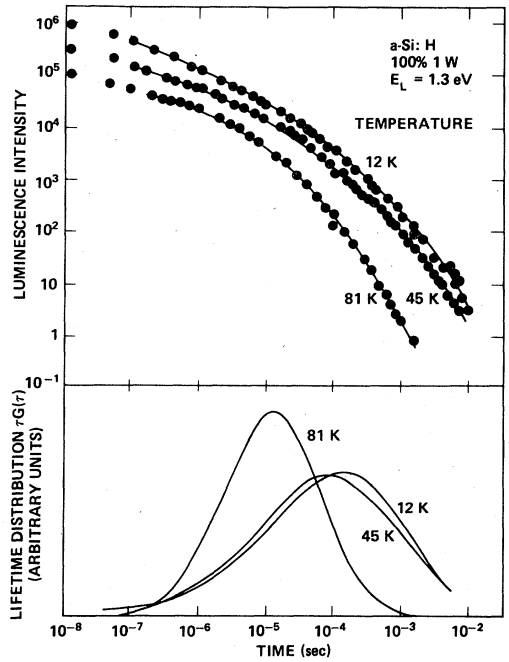

FIG. 4. Upper diagram (a) shows the decay of luminescence in response to a short excitation pulse (~20 nsec) at different temperatures. The lower diagram (b) shows the corresponding distribution functions $\tau G(\tau)$, normalized to the same value of $\int G(\tau)d\tau$. The solid lines in the upper diagram are the fits to the data obtained from the distribution functions.

these curves are constructed from about ten sets of data using differing time scales. These data are taken at a luminescence energy of 1.3 eV. Measurement at a higher energy tends to enhance the fast decay at the expense of the slow, as is described in more detail in Sec. III C. For most of the decay, the data is independent of the excitation intensity, as reported previously. However for measurements of time constants of 1–10 msec, using excitation pulses of 100 μsec or longer an intensity dependence is observed and this feature of the decay is discussed further in Sec. III D. As far as possible, Fig. 4 represents the low intensity limit.

The distribution of decay times $G(\tau)$ is obtained from the data of Fig. 4(a) as described in Sec. II. Figure 4(b) shows the function $\tau G(\tau)$ for the three measurement temperatures. The solid lines in Fig. 4(a) are the fits to the experimental data obtained from these $G(\tau)$. In each case an accurate fit is obtained except below 100 nsec. The function $\tau G(\tau)$ is chosen because of the logarithmic time scale, since

$$G(\tau)d\tau \equiv \tau G(\tau)d(\ln\tau). \tag{9}$$

The most striking feature of the decay data is that the distribution of lifetimes extends over more than five orders of magnitude in time. As is well known, the observed lifetime can be a combination of both radiative and competing nonradiative rates:

$$\tau^{-1} = P_r + P_{nr}. \tag{10}$$

Thus our estimate of the low temperature quantum efficiency implies that the radiative component differs from the observed values by at most a factor 2–4, Since this is a relatively small factor compared to the width of the distribution, it is clear that the data provide a reasonable approximation for the radiative rate. Furthermore we have already shown in Fig. 2 that the nonradiative component is mostly evident at times less than 10 μsec, so that the distribution at longer times should be an accurate description of the radiative component. In the discussion of the data in Sec. IV we therefore neglect any nonradiative components.

C. Spectral dependence of the decay

To observe the spectral dependence of the decay, it is convenient to measure time-resolved luminescence spectra, and some examples are shown in Fig. 5. There is a systematic shift of the spectrum to low energy by about 0.15 eV as the delay time after excitation is increased. However there is no discernible change in the shape of the spec-

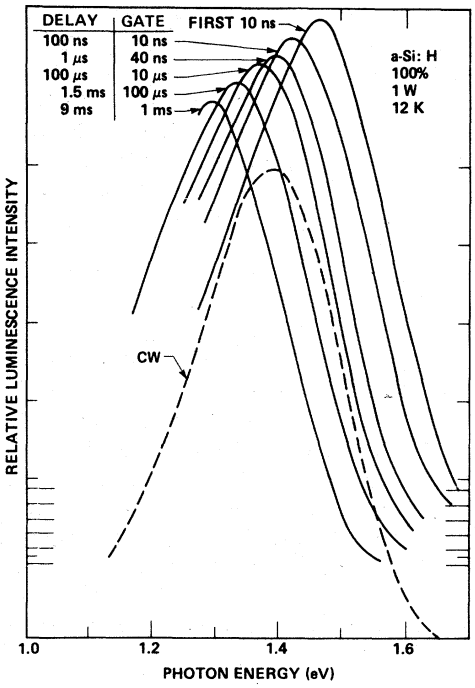

FIG. 5. Time-resolved luminescence spectra for delay times between 10^{-8} and 10^{-2} sec. The data at 1.5 msec is measured with a Si photodiode, whilst the remainder use a photomultiplier. The cw luminescence spectrum is also shown for comparison.

trum. The cw spectrum measured for the same excitation photon energy lies, as expected, within the set of time-resolved spectra. The energy of the luminescence peak of the time-resolved spectra are plotted as a function of delay time in Fig. 6. It is evident that the time-resolved shift can be separated into two components. First there is a shift that starts within the time resolution of the apparatus, and continues until about 1 μsec. Then the spectrum is almost unchanged up to 100 μsec.

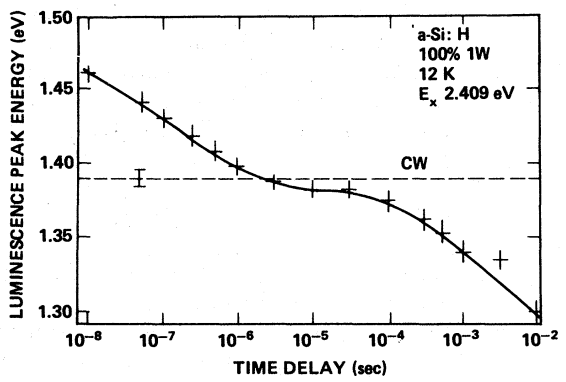

FIG. 6. Peak energies of the time resolved luminescence spectra and the cw spectrum, from the data of Fig. 5.

Finally at longer times there is a further shift of the peak to low energy. The time-resolved shift of the peak is smaller than the width of the luminescence line, and therefore the shift has only a small effect on the overall decay data. For example, it can be seen in Fig. 5 that at 1.3 eV, the intensity of both the fastest and slowest time-resolved spectra are within a factor of 2 of their peak intensity. This factor of 2 has to be compared with an intensity change of 10^6 over the whole decay curves of Fig. 4(a). We also note that the present data do not conflict with our previous measurements that found no spectral dependence of the decay except near 1.5 eV.[10] Those measurements were restricted to times less than 50 μsec, and so are dominated by the flat region of the data in Fig. 6.

D. Intensity dependence of the decay

Previous measurements also found that the decay is independent of the excitation intensity, from which it is deduced that the decay is monomolecular. We now show that this result is modified when long pulses and long decay times are involved. Figure 7 illustrates the luminescence decay after a 5-msec pulse and its dependence on excitation intensity. As the intensity increases, the decay gets faster, and the effect is particularly strong just after the end of excitation. The experiments use laser intensities of less than 1 mW (with a 1-mm^2 spot size) so that sample heating is insignificant. Also the total luminescence

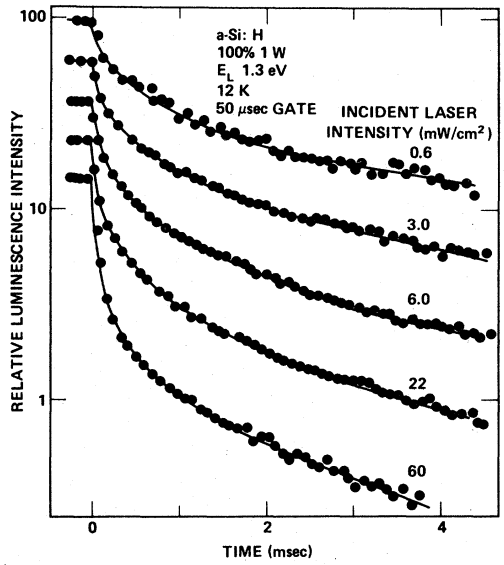

FIG. 7. Dependence of the luminescence decay after a 5-msec excitation pulse, on the incident laser intensity. At the excitation wavelength (5145 Å), the 10-K absorption coefficient is 1.2×10^5 cm^{-1}.

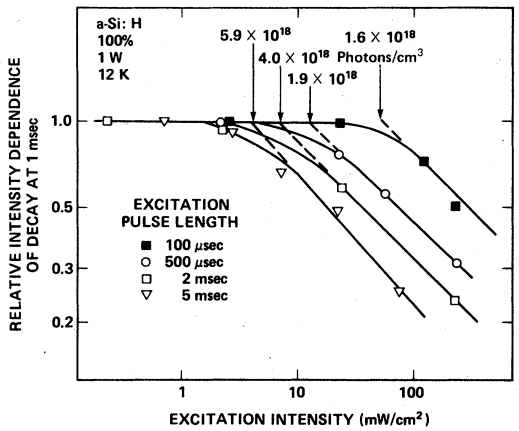

FIG. 8. Plot of the relative luminescence intensity after a decay time of 1 msec, vs the excitation intensity showing the onset of an intensity dependent decay, for different pulse lengths. The transition between the two regimes is defined by extrapolating the high intensity data as shown. The excitation densities (photon/cm^3) at the transitions are indicated.

intensity remains proportional to the excitation intensity. As a measure of the intensity dependence of the decay we compare the relative decay of luminescence after 1 msec. In Fig. 8 the data of Fig. 7, and data for other excitation pulse lengths is compared. We find that for each pulse length there is a low intensity region where the decay is unchanged and a high intensity region where it varies. It can be seen that as the excitation pulse length increases, the intensity at which the decay becomes intensity dependent decreases. Thus the reason why our previous measurements did not observe this effect is that the maximum pulse length used was only 5 μsec. The data of Fig. 8 suggest an intensity of more than 2 W/cm^2 would then be needed to observe the intensity dependence, and such high excitation power was never used in those measurements.

At 5145 Å, the 10-K absorption coefficient of the sample is measured to be 1.2×10^5 cm^{-1}. Therefore, assuming an absorption length of 825 Å the total density of absorbed photons for each pulse length was calculated, and is indicated in Fig. 8 for the point at which the data begins to show an intensity dependence. From the distribution of lifetimes $G(\tau)$ we can then calculate the density of electron-hole pairs at the end of the pulse, by integrating Eq. (1) over the known distribution. We find that the onset of the intensity dependence occurs at approximately the same pair density for each pulse length, the value being 1.5×10^{18} cm^{-3}. Allowing for the nonuniform illumination (due to absorption) and the uncertain effect of nonradiative recombination, this value is probably accurate to no better than a factor of 2. For a random distribution of electron-hole pairs of density N, the mean separation is approximately $(3/4\pi N)^{1/3}$. Thus the onset of the intensity dependence of the decay occurs at a pair separation of ~55 Å with an anticipated uncertainty of 20%–30%.

E. Temperature dependence

Figure 4 contains examples of the temperature dependence of the decay and of $\tau G(\tau)$. As the temperature increases the peak of the distribution shifts to lower τ and above 45 K the width of the distribution decreases. In Fig. 9 the reduction of the slow decay components as the temperature increases is shown in more detail. We have also investigated the temperature dependence of the cw luminescence intensity, in order to determine whether the observed change is due to the radiative or nonradiative component of the decay. Figure 10(a) shows the variation of luminescence intensity up to 150 K. The measurements are performed at a fixed luminescence energy near the peak of the spectrum, and the results are corrected for the change in the shape and position of the spectrum (see Fig. 11). Thus the data represent the total luminescence output. As reported previously[5] for a sample of somewhat lower efficiency, the luminescence intensity increases by nearly a factor of 2 up to 50 K. Above 50 K the intensity decreases, and in Fig. 10(b) the data are plotted as I_0/I-1 vs $1/T$, with I_0 taken

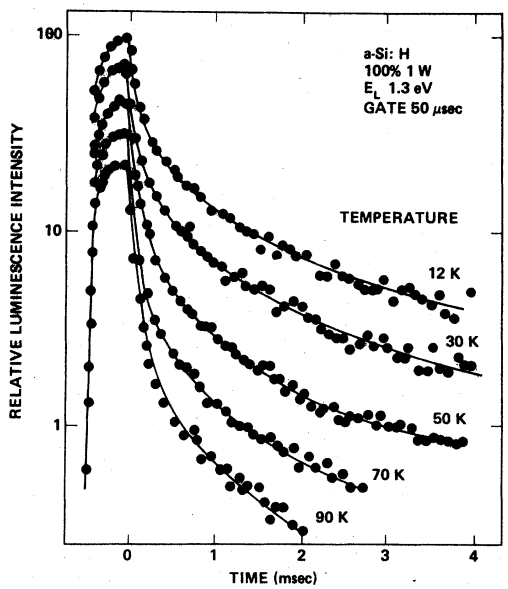

FIG. 9. Illustrating the temperature dependence of slow decay components, showing that there is a decrease in $\bar{\tau}$ between 12 and 90 K.

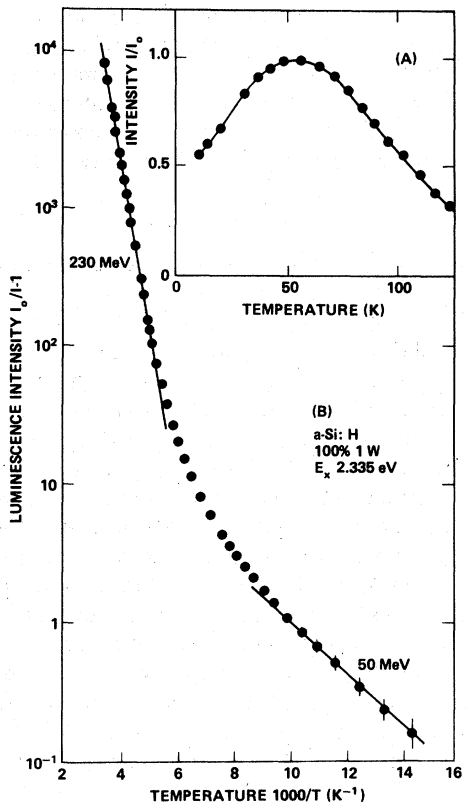

FIG. 10. Temperature dependence of the total cw luminescence intensity, showing the low temperature increase in (a) and the high temperature decrease in (b). Note the different vertical scales in (a) and (b). The error bars in (b) represent a 10% change in I_0.

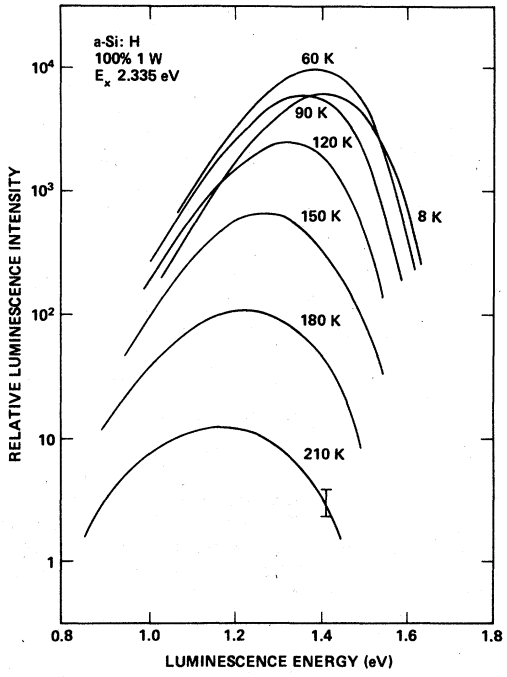

FIG. 11. Luminescence spectra at various temperatures plotted on a logarithmic scale showing the rapid decrease in intensity above 60 K, the shift of the peak to low energy.

as the intensity at 50 K. The resulting curve has an activation energy of ~50 meV at 100 K, increasing to 230 meV at 250 K. These results are very similar to other reports[13,14] except that we find a larger high-temperature activation energy. Between 10 K and 50 K, the increase in the luminescence intensity implies a decrease in the ratio of the nonradiative to radiative contributions. However a decrease in the nonradiative rate would lead to an increase in the measured decay times, contrary to observation. Thus we conclude that the faster decay must be due to an increase in the radiative recombination rate, at least for temperatures up to about 80 K. At higher temperatures, the strong thermal quenching probably dominates the decay through the nonradiative channel.

Figure 11 shows examples of the luminescence spectrum at different temperatures, plotted on a logarithmic scale, showing the relative intensity of the emission. As also reported by Austin *et al.*,[14] the peak shifts rapidly to low energy, and the width increases with temperature. Figure 12 contains plots of the temperature dependence of both the peak position and linewidth. Data are shown for two samples at differing excitation photon energies. Above 50 K the peak energies are identical. However below 50 K the curves diverge, and a weak dependence on the excitation energy is evident, a lower energy resulting in a higher energy of the luminescence peak. In Fig. 12(b) the linewidths are shown for the same samples and excitation conditions. Below 150 K the linewidths are independent of temperature, but depend on the sample and the excitation energy. Above 150 K the widths increase rapidly and are apparently identical for the three sets of data. Also shown in Fig. 12 is the temperature dependence of the absorption edge at two absorption coefficients. It can be seen that the temperature shift of the edge is smaller than the shift of the luminescence peak energy by about a factor of 5, and that at least up to 300 K, the slope of the absorption edge changes very little. As pointed out by Austin *et al.*,[14] the temperature dependence of the linewidth cannot readily be explained by phonon in interactions, without unreasonable values for the phonon energy. The much smaller temperature dependence of the absorption edge slope also argues against this model, since it is believed that phonon broadening is at least partially responsible

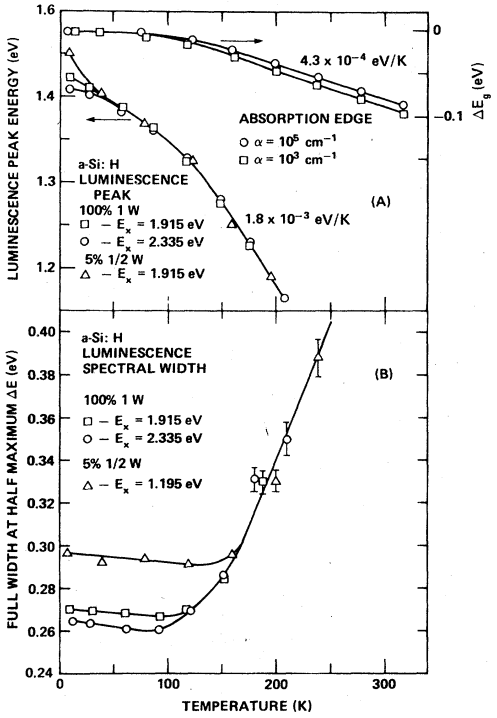

FIG. 12. (a) Temperature dependence of the luminescence peak energy, and of the absorption edge. The shift in the luminescence is much larger than that of the edge. Below 50 K the luminescence peak position depends on sample preparation and excitation wavelength. (b) Temperature dependence of the luminescence spectral width showing a rapid increase above 150 K, and low-temperature values that depend on sample preparation and excitation wavelength.

for the slope of the absorption edge.[5] A possible explanation of the temperature dependence of the spectral shape is given below.

IV. DISCUSSION

A. Decay measurements

Previous measurements of luminescence decay in doped and undoped a-Si:H indicate that the radiative decay is observed at times in excess of 10 μsec in all samples whilst the nonradiative mechanism is responsible for a fast initial decay whose magnitude increases as the luminescence efficiency decreases.[10] Figures 1 and 2 demonstrate this correlation for a series of undoped samples whose relative quantum efficiencies span two decades and confirm this interpretation of the decay. In the sample selected for study, which has a maximum quantum efficiency in the range 50%–100%, the decay at 10 K has a distribution of lifetimes that extend from 10^{-8} sec up to 10^{-2} sec with a mean lifetime defined by Eq. (8) of approximately 10^{-3} sec. The high quantum efficiency of this sample ensures that the observed distribution represents closely the radiative rates. The mean radiative lifetime of $\sim 10^{-3}$ sec compares with previous estimates of 10^{-8} sec[1] and 3×10^{-5} sec.[10] As the analysis of Sec. II shows, the response to pulsed excitation for a distribution of decay times can be deceptive as it strongly enhances the effect of the short time constant components. We emphasize that complete decay curves are required before a reasonable estimate of $\bar{\tau}$ can be deduced. The predominance of the long decay components can be seen in Fig. 7 which shows the response to a long excitation pulse. In the low excitation power regime, the intensity has dropped by less than a factor of 3 at 1 msec after excitation.

We interpret the luminescence in a-Si:H at 1.3–1.4 eV as originating from a transition between electrons and holes in band-tail states.[4-6] Mott[15] has pointed out that the thermalization of an electron hole pair into their lowest-energy level depends on two conflicting considerations. On the one hand, the Coulomb interaction is maximized if the pair overlaps strongly forming an "exciton". On the other hand, the carriers can lower their energy by thermalizing down the band tails. However since they then occupy levels with a smaller density of states, the mean separation of the electron and hole increases, reducing the Coulomb interaction. Whether the exciton or the separated pair represents the lowest-energy configuration depends on the relative magnitude of the Coulomb energy of the exciton compared with the width of the band tail.

The radiative recombination rate of the exciton-like configuration is expected to be [10,15]

$$\tau = \tau_0 M^3 , \tag{11}$$

where M is the ratio (≤ 1) of the electron and hole wave-function radii. The equivalent rate for an electron and hole separated by R with weak overlap is[16]

$$\tau = \tau_0 \exp\,(2R/R_0) , \tag{12}$$

where R_0 is the radius of the larger wavefunction. τ_0 is determined by the oscillator strength and the spin selection rules. No orbital selection rules are expected to apply to an amorphous semiconductor. Recent studies of spin-dependent luminescence[17] and magnetic properties[18] indicate that the transition in zero magnetic field is not strongly forbidden by spin, and thus we take $\tau_0 \sim 10^{-8}$ sec. To account for the observed decay within the exciton model requires $M \sim 10^2$, which is an order of magnitude larger than might reasonably be anticipated. On the other hand, large values of τ can easily result from Eq. (12) if the carriers are well

separated. The similarity of the second mechanism and donor-acceptor (*D-A*) pair recombination has already been noted,[14] and it is well known that very long lifetimes, even in excess of 1 sec, are observed from *D-A* pairs due to weak overlap.[16] We therefore conclude that the magnitude and distribution of τ rules out the exciton model for most recombination events, and that radiative tunneling occurs instead. According to the recombination model described by Eq. (12) the distribution of pair separations R corresponds to the distribution of $\ln\tau$. Thus the measurements of $\tau\, G(\tau)$ shown in Fig. 4 give directly that the most probable value of R/R_0 is ~5 and that the half width of the distribution of R/R_0 is ~2.

The model of radiative tunneling implies that the width of localized states at the band edge is greater than the exciton binding energy which has been estimated to be ~0.1 eV.[1] An estimate of the magnitude of band tailing can also be obtained from the luminescence data. Time-resolved spectra show a montonic shift of the peak to low energy by ~0.15 eV with increasing time after excitation while no change is observed in the shape of the spectra. These observations are consistent with a model in which the major contribution to the linewidth is the electron-phonon interaction, as identified from excitation spectra measurements.[5] The distribution of zero-phonon energies is a smaller effect and is responsible for the shifts in the time-resolved spectra. We conclude that the observed shift of 0.15 eV is a measure of the band tailing,[6] because carriers in extended states above the mobility edge are expected to have a thermalization time much smaller than the time resolution of our experiments. A more detailed discussion of the time-resolved spectra is given in Sec. IV B.

It was reported previously that the decay curves are independent of the excitation intensity and therefore that the recombination kinetics are monomolecular.[10] By extending the experiments to larger times using longer excitation pulses, we observe a departure from the monomolecular behavior as shown in Figs. 7 and 8. The onset of an intensity-dependent decay occurs when the density of excited electron-hole pairs exceeds ~1.5 $\times 10^{18}$ cm^{-3}. The result is the same whether this density is achieved with a short intense pulse or a longer weaker pulse. Two explanations of the effect seem possible. Firstly, the high intensity may saturate the available low-energy states with slow decay, forcing electron-hole pairs to occupy higher-energy states with faster decay times. A consequence of this model is that the spectrum should shift to higher energy as the intensity increases. In practice, a very small shift is observed (Fig. 13) but it is only about 10 meV, and it is doubtful whether this is sufficient to account for the large change in τ.

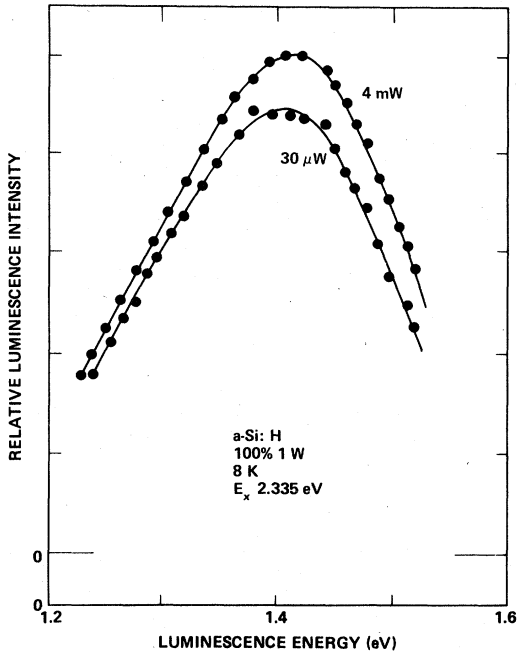

FIG. 13. Luminescence spectra of a sample at two different excitation intensities. There is a very small shift of the peak to higher energy by ~10 meV as the intensity increases. The illuminated area was 4 mm^2 and the intensity is such that sample heating should be negligible.

The second explanation is that there is a transition to bimolecular recombination. Monomolecular kinetics are assumed to occur because electrons and holes recombine geminately. The justification of this model is that the electron and hole will diffuse apart only a short distance during thermalization, and once they occupy tail states they are not expected to diffuse further if the temperature is sufficiently low. As described in Sec. IV D, the absence of large scale diffusion is clearly indicated by the decay data. However, if the excitation intensity is such that the mean distance between pairs is less than the electron-hole separation of a pair, then an electron has several holes available for recombination, and the kinetics will be bimolecular. The transition to an intensity dependent decay occurs at a density when the mean separation of pairs is 55 Å. Since we find that the mean electron-hole separation of a pair is $5R_0$, we conclude that the average value of R_0 is 11 Å. This wave-function radius is a reasonable estimate for a band tail and in fact agrees with our previous estimate of 12 Å based on nonradiative transitions to defect states with spin.[4]

Fortunately, the explanation based on the saturation of tail states leads to an identical value of R_0. The argument is that saturation will only effect the decay if the majority of the radiative transitions occur from the saturated states. Thus the onset of saturation at a pair density of 1.5×10^{18} cm^{-3} implies a mean electron-hole separation of 55 Å and a wave-function radius of 11 Å as before.

Figure 7 shows that the intensity-dependent regime is obtained with an excitation intensity of 3 mW/cm^2 at 5145 Å and a 5-msec pulse. This low power means that cw measurements of the spectra can easily operate in this regime, and the possibility of bimolecular recombination should not be overlooked.

B. Time-resolved spectra

The time-resolved shift of the luminescence spectrum demonstrates that there is a distribution of zero-phonon energies contributing to the recombination of at least 0.15 eV. There are two plausible mechanisms for the time-resolved shift of the spectrum, which we refer to as thermalization and localization:

(a) Thermalization. After photoexcitation the electrons and holes are excited well above the band edge, and they will thermalize before recombining. It is expected that thermalization within the extended states will occur within ~10^{-12} sec.[19] However once the carriers reach the localized states below the mobility edge, further thermalization will be by tunneling which can be much slower. The tunneling rate depends on the available density of states, and is expected to decrease exponentially as the carriers drop deeper into the tail states. If radiative recombination occurs before thermalization is complete, then the motion of the carriers down the band tails will be observed as a time-resolved shift of the luminescence.

(b) Localization. Even if thermalization is complete, a time-resolved shift of the spectrum can be observed if the luminescence energy is correlated with the decay time. The lifetime of a pair recombining by radiative tunneling depends exponentially on R/R_0 where R is the electron-hole separation and R_0 is the radius of the larger wavefunction. Since the radius of a localized state decreases as the binding energy increases, the lowest energy pairs will have the longest decay times. In general we expect this mechanism to be prevalent at long decay times, since a shift in the spectrum will only be observed after a sufficient fraction of states with small R/R_0 have decayed.

The experimental data show two regimes in the time-resolved shift of the spectrum, and we suggest that both mechanisms occur. We interpret the fast component of the shift, at times less than 1 μsec, as thermalization. The initial excitation energy is at 2.4 eV so that the measurements (Fig. 6) observe only the final 0.07 eV out of a total energy loss of 1.0 eV. This is consistent with the expectation that most of the thermalization will occur faster than the time resolution of our apparatus. Davis[19] has estimated that in selenium during thermalization the electron-hole pair separates to about 40 Å for 1 eV of excess energy. Similar estimates for silicon result in a smaller value.[1] Nevertheless we believe that the observed separation of ~55 Å is consistent with thermalization. The Davis model also predicts that the separation, and therefore the radiative lifetime depends on the excitation energy. We have not attempted to confirm this directly, but we do observe (Fig. 12) that at 10 K, cw excitation at 6471 Å results in a luminescence peak at slightly higher energy than with excitation at 5309 Å. We suggest the reason is that the electron-hole pair is less separated and so recombines with a higher efficiency during thermalization, giving an enhanced high-energy contribution to the spectrum. It is reported elsewhere[6] that the position of the spectrum is sensitive to the excitation method because of different thermalization properties. We also note that since thermalization apparently continues up to ~1 μsec, tunneling from site to site in the tail states may dominate the separation of the electron-hole pair. In this case no dependence of the decay on the excitation energy is expected. Experiment might resolve this point.

It seems extremely unlikely that the time-resolved shift of the spectrum between 100 μsec and 10 msec can be explained by thermalization because of the very long times involved. Instead we interpret this region as originating from the decrease in R_0 with increasing binding energy of the carriers. The range of decay times involved indicates about a 40% variation in R_0. An interesting feature of the time-resolved spectra is that the spectral linewidth is independent of time, within the experimental uncertainty. The broad line results from an electron-phonon coupling, and it is to be expected that the strength of the coupling would increase with the binding energy of the carriers. In Sec. IV E we argue that only holes are self-trapped, and electrons are not strongly coupled. Thus a possible explanation of the time resolved spectra is that holes are self-trapped very rapidly, and that virtually all the shift of the spectrum originates from the electron

energy. In this case the conduction band tail would have an estimated width of 0.15 eV, which is in good agreement with other estimates.[20]

C. Temperature dependence

Above about 60 K the luminescence efficiency in a-Si:H decreases strongly, which is generally attributed to the activated diffusion apart of electron-hole pairs. It is also found (Fig. 10) that at lower temperature, between 10 and 50 K, the luminescence efficiency increases by about a factor of 2. Lifetime measurements show that between 10 and 50 K the decay lifetime decreases. Clearly, therefore, the radiative rate is increasing since the reduced nonradiative contribution can only increase τ. Furthermore, even at higher temperatures, the decrease in τ cannot be fully explained by the nonradiative decay. For example, at 80 K the peak of $\tau G(\tau)$ has decreased by more than an order of magnitude while the luminescence is only 20% below its peak. However, above 100 K, when the luminescence intensity decreases strongly the nonradiative transition presumably dominates the decay.

One proposed mechanism for the low-temperature increase in efficiency is that the barrier to self-trapping is more easily overcome.[5] However, since this process does not compete with the radiative decay, no change in the decay time should be observed. Thus the decrease in τ appears to rule out this interpretation. The mechanism of radiative tunneling is itself not expected to give a temperature-dependent recombination rate. We suggest instead that both the high-temperature quenching and the low-temperature enhancing may be due to carrier diffusion based on the Onsager model.[19,21] It is well known that the diffusive motion of an electron-hole pair is such that at low temperature ($T<T_c$) the electron and hole tend to come together, whilst at high temperature ($T>T_c$) they move apart. If in addition the diffusion rate is thermally activated, then at very low temperature there will be no motion at all. Thus we suppose that below 10 K there is no carrier motion; between 10 and 50 K the pair has an increasing tendency to move together, enhancing the radiative rate; and above 50 K the pair separates and recombines nonradiatively. The transition temperature T_c is given by

$$kT_c = e^2/8\pi\epsilon\epsilon_0 R. \tag{13}$$

Our estimate of $R \sim 50$ Å gives $T_c \sim 150$ K which is larger than that observed, but possibly the Coulomb interaction is partially screened. A further discussion of the influence of carrier diffusion on the low-temperature decay is given in Sec. IV D.

The luminescence peak energy shifts rapidly to low energy with increasing temperature (Fig. 12). This shift cannot be explained by the temperature dependence of the band gap which is about five times smaller. The linewidth also increases rapidly above 150 K, suggesting a phonon mechanism. However, both effects are larger than can reasonably be explained by phonon broadening. Instead we interpret these observations as a further consequence of the distribution of zero-phonon energies. If thermal quenching is due to activated carrier diffusion, then the electrons and holes furthest down the band tails will require the highest temperature for release and will correspond to the lowest-energy luminescence. It can be seen in Fig. 11 that at an energy of, say 1.0 eV, thermal quenching is not significant until 120–150 K. According to this interpretation of the temperature dependence, the activation energy for quenching at any temperature should roughly equal the shift of the luminescence peak from its low temperature value. A comparison of Figs. 10 and 12 shows that this is indeed the case. We further suggest that the increase in line broadening above 150 K originates because thermal excitation of the self-trapped carrier can also occur. Carriers with the largest electron-phonon coupling will necessarily have the largest binding energy. From the temperature-dependence data of Fig. 12, we deduce a distribution of zero-phonon energies extending 0.2–0.25 eV (allowing for the shift of the band gap and the increased electron-phonon coupling). This distribution is greater than that observed in time-resolved spectra possibly because in this experiment there is a contribution from both electrons and holes.

D. Influence of diffusion

The initial discussion of the decay data assumed that at low temperature, electrons and holes are immobile after thermalization and recombine either radiatively or nonradiatively by a single tunnelling step. At elevated temperatures, the reduced radiative rate indicates that diffusion is possibly significant. Here we discuss in more detail the evidence for diffusion and its contribution to the radiative decay. It is clear that at least up to 80 K, diffusion over distances much greater than the pair separation does not occur. The reason is that if, for example, an electron occupies many different sites during its lifetime, then the observed decay will be a spatial average which should be the same for all electrons. Instead, the observed decay times are widely distributed. However, diffusion over a limited dis-

tance is possible and Hong and Noolandi have discussed its effect on the recombination rate of the Onsager model.[22] Three distances are important in this problem; first, R, the separation of the electron and hole after thermalization; second, the Onsager radius R_0 defined by Eq. 13; and thirdly, the recombination radius R_1 defined such that when $R < R_1$ the recombination rate exceeds the diffusion rate. As noted before, at low temperature R_0 is large and diffusion apart of carriers is negligible. The importance of diffusion depends on the relative magnitude of R and R_1. Calculations show[22] that for $R > R_1$, the onset of luminescence after an excitation pulse should be delayed by a time of the same magnitude as the observed decay time because of the requirement that the carriers diffuse together to the distance R_1. No such delay is observed within an experimental time resolution of 10^{-8} sec. Since the low-temperature data can be explained satisfactorily without diffusion, we conclude that there is no evidence for the dominance of diffusion. On the other hand, there is evidence for its significance at higher temperatures.

E. Model for recombination in *a*-Si:H

In this section, we attempt to relate the results of this investigation to the general models for electronic transitions in *a*-Si:H. One important issue is the role of the electron-phonon interaction of the electron and hole. The decay data show that during recombination the electron and hole are well separated and overlap weakly. Thus we infer that the observed phonon coupling must apply to the individual particles, and that there is a negligible contribution from the electron-hole interaction. Nevertheless, we also find that one of the carriers has a wave function of radius ~11 Å. This size seems to be incompatible with strong self-trapping. Therefore we conclude that only one of the carriers is strongly coupled.

Strong coupling of a carrier in a band tail state does not necessarily imply polaron formation of all the carriers in the band. Mott and Stoneham[23] have shown that a molecular polaron has a barrier to self-trapping and that the barrier decreases if the state is localized before self-trapping occurs. Thus it is plausible that self-trapping only occurs at a fairly small density (e.g., 10^{20} cm^{-3}) of localized states within the band tail, and that the remaining states in the band are uncoupled. We propose that holes are self-trapped in this way and that electrons do not couple strongly. A density-of-states diagram illustrating this model is shown in Fig. 14(a). The self-trapped hole band is shown split off from the valence-band tail by the distortion energy W_p. In transport experiments we expect this type of self-trapped state to act as a hole trap because the relatively large separation would suppress polaron hopping. The evidence for our model that can be obtained from experiments other than luminescence is as follows: (1) Electrons are more mobile than holes.[20,24] Transport measurements have been interpreted as electron motion in a band tail of width ~0.15 eV, and the wave-function radius is generally estimated to be 10–20 Å. (b) Holes have a low mobility with an activation energy ~0.25–0.35 eV.[24] A distortion energy of ~0.2–0.25 eV and an additional localization energy of ~0.1 eV would account for this result. (c) We have shown that nonradiative transitions occur by tunneling of the larger wave-function particle into deep states and that these transitions predominate if the density of states exceeds ~10^{17} cm^{-3}.[4] Field effect measurements[25] show that samples with high luminescence efficiency have a density of states of at least 10^{19} cm^{-3} ~0.3–0.4 eV above the valence-band mobility edge but a much smaller density of electron traps.

Figure 14(b) illustrates the density of gap states derived from field effect measurements by the

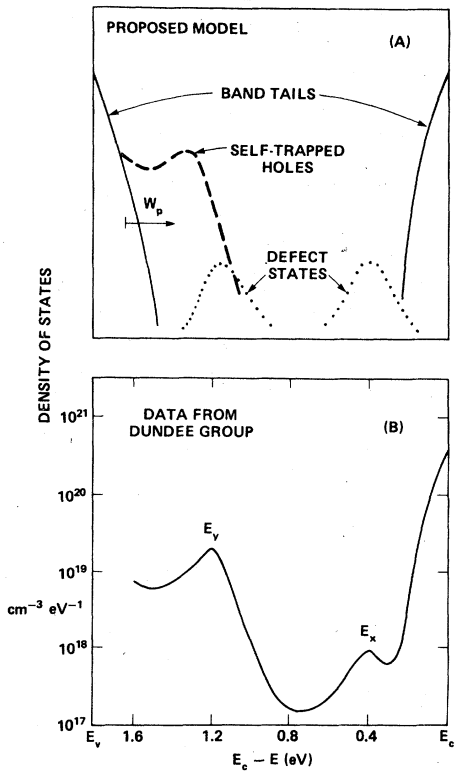

FIG. 14. (a) Model density of states diagram, illustrating band-tail states, self-trapped hole states split off from the valence-band tail, and defect states. (b) A typical density of states obtained from field effect measurements by the Dundee group (Ref. 25).

Dundee group.[25] The applicability of this data to our results is uncertain because their samples are prepared under different conditions. However, those samples also show efficient luminescence, with apparently similar decay properties, although the luminescence peak is at a lower energy than in our samples.[2,14] We therefore expect that the same general features are present in the density of states of our samples. We note also that Singh and Cohen[26] have reanalyzed the Dundee field effect data and conclude that the electron trap E_x has a smaller density of states and a larger binding energy than is shown in Fig. 14(b). It is not clear whether that analysis also modifies the peak E_y.

The qualitative similarity between Figs. 14(a) and 14(b) leads us to suggest that the peak E_y is in fact the self-trapped hole band. Spear originally considered that both E_x and E_y are different charge states of a single defect.[27] However the large difference in density of states that subsequently became apparent[25] precludes this possibility. We assume that E_x is indeed a defect state, and that any corresponding hole trap for the defect makes only a minor contribution to E_y [see Fig. 14(a)].

Of the many possible electronically active defects in a-Si:H, the two most frequently discussed are the divacancy (or small void) and the dangling bond. In the divacancy, bond reconstruction is assumed to occur so that the neutral defect contains paired electrons. On the other hand the neutral dangling bond contains an unpaired electron. These types of defect are therefore distinguishable by their ESR activity. It has been shown that the luminescence efficiency of different a-Si:H samples is correlated with the observed spin density.[4] It was also deduced that nonradiative recombination was by tunneling to localized states in the gap, and that the spin density N_s was at least proportional to the defect state density N_D;

$$N_s = \beta N_D \,. \tag{14}$$

The wave-function radius of the tunneling particle was found to be $12\beta^{-1/3}$ Å. In this study we obtain a radius of 11 Å ±20% and therefore conclude that $\beta \sim 1$. Thus we find that essentially all the nonradiative centers are traps with unpaired electrons. However even this result is not yet sufficient to identify the E_x centers. In a recent paper on photoconductivity, Anderson and Spear[28] propose that nonradiative recombination in undoped material is by capture of an electron by a positively charged trap near the Fermi energy, and that the neutral E_x are not significant as recombination centers despite their larger density of states. The justification for this model is that the capture cross section for a charged state can be many orders of magnitude larger than for a neutral state. However in luminescence at low temperature, capture is by tunneling rather than by diffusion and there will be little to distinguish charged and neutral states. This result indicates that the singly occupied electron traps that dominate nonradiative recombination at low temperature are the majority of electron traps and so can be identified with the states E_x. These states therefore have the spin properties of dangling bonds and the total density of states of E_x from Fig. 14(b) is $\sim 10^{17}$ cm^{-3} (based on the analyses of Singh and Cohen the density is $\sim 10^{16}$ cm^{-3}). In our previous measurements correlating luminescence intensity with spin density,[4] we found that samples with $\leq 10^{17}$ cm^{-3} spins had high luminescence efficiencies. Thus, according to this model, the field effect data is completely consistent with samples having a high luminescence efficiency.

V. CONCLUSIONS

The principal results obtained in the study are as follows:

(a) In undoped a-Si:H samples covering a wide range of luminescence quantum efficiencies, both radiative and nonradiative recombination is observed. The correlation of the rates for the two transitions with the cw luminescence intensity, provides further confirmation of a model in which the electron-hole pair recombines radiatively unless it is excited within some critical distance from a defect.

(b) The radiative decay time constant has a distribution extending from 10^{-8} to 10^{-2} sec. The extremely broad distribution and the long decay times are indicative of a radiative tunneling mechanism.

(c) When the electron-hole pair density exceeds about 1.5×10^{18} cm^{-3}, the decay becomes excitation-energy dependent. The reason is probably that at high pair densities, the recombination is no longer geminate, and the decay kinetics become bimolecular. The critical pair density corresponds to an average pair separation of ~55 Å. Combining this result with the distribution of decay times, we obtain a tunneling parameter for the radiative recombination which corresponds to a wave-function radius of 11 Å ± 20%.

(d) Time-resolved spectra exhibit a shift to low energy of ~0.15 eV over the investigated time scale (10^{-8}–10^{-2} sec). The spectral shift is explained by carrier thermalization at times less than 10^{-6} sec, and by the relation between the wave-function radius and binding energy of carriers, at times greater than 10^{-4} sec. The shift of 0.15 eV is due to a distribution in the zero-phonon recombination energies, and is thought to

originate from band tailing.

(e) The temperature dependence of the decay and and of the cw luminescence intensity is seen as evidence of thermally activated carrier diffusion. Between 10 and 50 K, the increase in luminescence intensity and the decrease in the decay times can be explained by diffusion together of an electron and hole under the Coulomb attraction. The thermal quenching above 50 K is explained by pair ionization.

(f) The large temperature-dependent shift of the luminescence peak energy is further evidence for a distribution of zero-phonon energies due to the width of the band tails.

(g) Based on a combination of the present data and transport measurements reported by other groups, we propose a model in which tail-state holes are self-trapped with a distortion energy of 0.2–0.25 eV, whilst electrons are not strongly coupled to the lattice. We tentatively identify the self-trapped holes with the E_y band reported in the field effect density of states. Finally, the data suggest that over the specific range of deposition conditions that we have investigated, the predominant defect is of the dangling bond type.

ACKNOWLEDGMENTS

The authors are grateful to D. K. Biegelsen, J. C. Knights, and J. Noolandi for useful discussions, and to J. C. Knights for providing samples.

---

*Present address: IBM Research Laboratory, San Jose, California.

[1]D. Engemann and R. Fischer, AIP Conf. Proc. 31, 37 (1976).
[2]T. S. Nashashibi, I. G. Austin, and T. M. Searle, Philos. Mag. 35, 831 (1977).
[3]J. I. Pankove and D. E. Carlson, *Proceedings of the Seventh International Conference on Amorphous and Liquid Semiconductors*, edited by W. E. Spear (Edinburgh University, City, 1977), p. 402.
[4]R. A. Street, J. C. Knights, and D. K. Biegelsen, Phys. Rev. B 18, 1880 (1978).
[5]R. A. Street, Philos. Mag. B 37, 35 (1978).
[6]R. A. Street, C. Tsang, and J. C. Knights, Proceedings of the Fourteenth International Conference on the Physics of Semiconductors, edited by B. L. H. Wilson (Institute of Physics, London, 1978), p. 1139.
[7]J. I. Pankove and D. E. Carlson, Appl. Phys. Lett. 29, 620 (1976).
[8]T. D. Moustakas, D. A. Anderson, and W. Paul, Solid State Commun. 23, 155 (1977).
[9]K. Morigaki, D. J. Dunstan, B. C. Cavenett, P. Dawson, and J. E. Nicholls, Solid State Commun. 26, 981 (1978).
[10]C. Tsang and R. A. Street, Philos. Mag. B 37, 601 (1978).
[11]J. C. Knights, AIP Conf. Proc. 31, 296 (1976).
[12]We are assuming that the decay kinetics are monomolecular and that the decay is not saturated. Our observations find that this assumption is applicable except at high excitation intensities and long excitation pulses (see Sec. III D).
[13]D. Engeman and R. Fischer, *Amorphous and Liquid Semiconductors*, edited by J. Stuke and W. Brenig (Taylor and Francis, London, 1974), p. 947.
[14]I. G. Austin, T. S. Nashashibi, and T. M. Searle, J. Non-Cryst. Solids (to be published).
[15]N. F. Mott, Philos. Mag. 36, 413 (1977).
[16]D. G. Thomas, J. J. Hopfield and W. M. Augustiniak, Phys. Rev. 140A, 202 (1965).
[17]D. K. Biegelsen, J. C. Knights, R. A. Street, C. Tsang and R. White, Philos. Mag. B 37, 477 (1978).
[18]R. A. Street, D. K. Biegelsen, J. C. Knights, C. Tsang, and R. White, Solid State Electronics 21, 1461 (1978).
[19]E. A. Davis, J. Non-Cryst. Solids 4, 107 (1970).
[20]P. G. LeComber, A. Madan, and W. E. Spear, J. Non-Cryst. Solids 11, 219 (1972).
[21]L. Onsager, Phys. Rev. 54, 554 (1938).
[22]K. M. Hong and J. Noolandi, J. Chem. Phys. 69, 5026 (1978).
[23]N. F. Mott and A. M. Stoneham, J. Phys. C 10, 339 (1977).
[24]A. R. Moore, Appl. Phys. Lett. 31, 762 (1977).
[25]A. Madan, P. G. LeComber, and W. E. Spear, J. Non-Cryst. Solids 20, 239 (1976); A. R. Madan and P. G. LeComber, Ref. 3, p. 377.
[26]J. Singh and M. Cohen, Phys. Rev. (to be published).
[27]W. E. Spear, Ref. 13, p. 1.
[28]D. A. Anderson and W. E. Spear, Philos. Mag. 36, 695 (1977).